INT. J. NUM. METH. HEAT FLUID FLOW, VOL. 6, NO. 7, 3–30 (1996)

FAST – A GENERALIZED FV SOLUTION OF CONVECTION-DIFFUSION PROBLEMS BY MEANS OF MONOTONIC v-SPLINES PROFILES

V. PENNATI†, M. MARELLI‡ AND L.M. DE BIASE‡

†ENEL SpA – CRIS, Via Ornato 90/14, 20162 Milano, Italy
‡University of Milano, Department of Mathematics, Via C. Saldini 50, 20133 Milano, Italy

ABSTRACT

In this paper new cubic v-splines monotonic one-dimensional profiles are presented, for the finite volume solution of convection-diffusion problems. By studying the profile in normalized variables, some weight functions have been determined for the profile. Being free of the requirement that the volumes be equal, the volume size can be reduced where needed. Numerical properties of the proposed method were formally analysed and are confirmed by numerical examples included here.

KEY WORDS Advection CFD Flux integral High order

INTRODUCTION

The requirement that the physical quantities in fluid dynamics laws be conserved lead, in recent years, to the introduction of finite volume methods (FV), which work with the integral form of the problem.

These methods require the computational domain to be subdivided in a finite number of control volumes such that their union covers the domain. Fluxes along a face of the control volume, moreover, must be computed by formulae independent of the volume itself; this, together with the assumption that, when overlapping volumes are chosen, each internal face belongs to two adjacent volumes, grants conservation since flux contributions on each internal volume and only two cancel when the domain is recomposed by summing fluxes relative to each volume.

The differential equation has to be integrated on each volume and this means evaluation of the integrals, volumes and areas; since, in general, physical quantities are assumed constant on each volume and on each face, a proper approximation of flux terms on the faces has to be determined[1].

Among the various methods in the literature, the most frequently adopted couple FV methods with finite difference formulae, with or without domain transformation[2-4], or with finite element methods[5-7].

Consider the one-dimensional unsteady convection-diffusion equation:

$$\frac{\partial \rho \Phi}{\partial t} = - \frac{\partial \rho u \Phi}{\partial x} + \frac{\partial}{\partial x}\left(\Gamma \frac{\partial \Phi}{\partial x} \right) + S \qquad (1)$$

where Φ is the dependent variable, $u(x,t)$ the convective velocity, ρ the density, Γ the diffusion coefficient and S the source term. By a FV technique, this equation is integrated in time between t and $t + \Delta t$ and in space on a control volume of size A (*Figure 1*):

This work was financially supported by ENEL SpA CRIS

0961–5539/96

Received June 1994
Revised December 1995

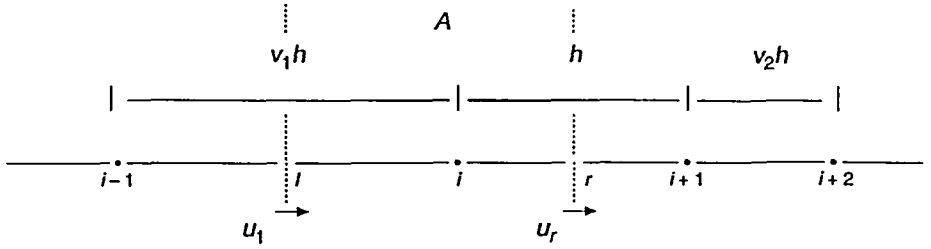

Figure 1 Control volume relative to node i with convective velocities $u_l, u_r > 0$

$$\rho_i \frac{\bar{\Phi}_i^{n+1} - \bar{\Phi}_i^n}{\Delta t} = \frac{\rho_l u_l \Phi_l^* - \rho_r u_r \Phi_r^*}{A} + \frac{\Gamma_r \left.\frac{\partial \Phi^*}{\partial x}\right|_r - \Gamma_l \left.\frac{\partial \Phi^*}{\partial x}\right|_l}{A} + S \quad (2)$$

where ~ stands for the spatial average,* for the temporal average and S is an average in both time and space of the source values. When discretizing equation (1) by a FV method, because of the presence of a convective flux, the choice of a profile by which variable Φ is assumed to follow some assigned local behaviour, which takes the velocity field into account, is very useful and effective.

For the definition of such a profile it is useful to have a grid of points together with the volumes. In fact the two subdivisions of the domain are strongly correlated: a definition of the grid gives rise to some criteria for the definition of the volumes and vice versa. For a coupling FD-FV, for example, the most frequent choice is the definition of an orthogonal cartesian grid and the positioning of the volume faces at mid-distances between grid points.

The simplest profile one can impose on variable Φ to evaluate it at the volume faces involves a linear interpolation of the values at two grid points adjacent to the face; this leads to Central Differencing Schemes (CDS), which, for high Peclet numbers ($Pe = uA/\Gamma$, $Pe \geq 2$), gives birth to spurious oscillations in the numerical solution.

In order to avoid this problem, an UPWIND profile (UDS) imposes variable Φ at a proper point on the volume face to take on the value it had in the upstream grid point with respect to the direction of the flux motion. By this approach the numerical solution has a more realistic physical behaviour, since the velocity vector is considered; there can arise, however, some false diffusion since the profile involves only one point at a time. There is also a reduced precision in 2 and 3 dimensions, due to the flux lines not being normal with respect to grid lines; when this happens a Skew Upstream Differencing Scheme or a Skew Upstream Weighted Differencing Scheme is therefore a better choice[8].

With an Exponential Differencing Scheme (EDS)[9,10], convective and diffusive fluxes are computed by using the solution, in closed form, of a 1D stationary problem without source terms. Although this scheme is very accurate for 1D problems, it is not used frequently because of its high computational cost, due to the computation of the exponentials included in the profile.

In order to avoid this cost (maintaining the quality of numerical results), the Power-Law scheme was introduced; this scheme combines the positive aspects of CDS and UDS by giving different values to the coefficients in the profile, according to a criterion based on Peclet number[11].

A difference scheme which proves very effective in dealing with convective terms is QUICK[12]; this scheme finds the value for a volume face by a quadratic interpolation using three points, two of which are in the upwind direction with respect to the motion direction on the face. For instance, considering face r of the control volume (*Figure 1*), we have:

$$\Phi_r = \frac{1}{2}(\Phi_i + \Phi_{i+1}) - \frac{\Phi_{i+1} - 2\Phi_i + \Phi_{i-1}}{8} \qquad u_r > 0 \qquad (3)$$

For the diffusive term a linear interpolation is used. The QUICK profile enjoys several advantages: the numerical diffusion is negligible, the algorithm is easily implemented and the computational cost is low. It gives, moreover, a local spatial truncation error of the second order for convection-diffusion equations, of the third order for pure convection problems.

Since this scheme was devised for problems with slow time variations, when used for highly unsteady problems it results with less accuracy, since its temporal truncation error is $O(\Delta t)$. For this kind of problems a modified version named QUICKEST is more advisable[13]; here temporal averages of equation (2) depend on the Courant number ($c = u\Delta t/A$). The profile on face r of the control volume is:

$$\Phi_r(c) = \Phi_r^{(2)} - \frac{(1-c^2)}{3!}\left(D_r^2 - \frac{SGN(c)}{2}\delta_r^3 \right)$$

with

$$2D_r^2 = \Phi_{i+2}^n - \Phi_{i+1}^n - \Phi_i^n + \Phi_{i-1}^n \qquad \delta_r^3 = \Phi_{i+2}^n - 3\Phi_{i+1}^n + 3\Phi_i^n - \Phi_{i-1}^n \qquad (4)$$

$$\Phi_r^{(2)} = \frac{1}{2}[(\Phi_i^n + \Phi_{i+1}^n) - c(\Phi_i^n - \Phi_{i+1}^n)]$$

Since QUICK and QUICKEST schemes were defined only for equal volumes, we thought it could be useful to introduce a cubic profile with the same numerical effectiveness but which could allow us to work with unequal volumes. Towards this end we adopted weighted cubic v-splines defined by means of three consecutive grid points[14].

In this paper we are proposing the introduction of some weighting functions in order that the profile we define for a 1D steady flow be monotonic; the resulting local spatial truncation error is of the third order for equal volumes, and reduces to the second at the faces which are not equidistant from the two adjacent grid points.

We stress that local monotonicity is extremely important if spurious oscillations in the numerical solution are to be avoided and that in our profile monotonicity is implied by the definition itself and not accomplished after some modification[15].

WEIGHTED CUBIC v-SPLINES

In this section we describe the construction of weighted cubic v-splines.

Given interval $[\overline{a},\overline{b}]$ and a partition $\overline{a} = x_1 < \ldots < x_n = \overline{b}$, let $\Phi_1, \ldots \Phi_n$ be the values to be approximated in such a way that $\Phi(x_i) = \Phi_i$, $i = 1,2, \ldots, n$. A weighted cubic v-spline is a piecewise cubic function of C^1 class, minimizing the functional

$$V(\Phi) = \int_{\overline{a}}^{\overline{b}} w(t)[\Phi''(t)]^2 \, dt + \sum_{i=1}^{n} s_i(\Phi'(t_i))^2 \qquad (5)$$

where $w(t)$ is an integrable function; we assume w to be piecewise constant and its value w_i on interval $[x_i, x_{i+1}]$ to give the weight for the interval itself, by which the curvature of the spline function can be controlled; s_i is a point weight yielding control of the first derivative at the nodes. The solution of the minimization problem above must also verify one of the following conditions:

(1) conditions on the first derivative:

$$\Phi'(\overline{a}) = m_1 \quad \text{and} \quad \Phi'(\overline{b}) = m_2$$

(2) natural conditions:

$$w_1\Phi''(\bar{a})-s_1\Phi'(\bar{a})=0 \quad \text{and} \quad w_{n-1}\Phi''(\bar{b})+s_n\Phi'(\bar{b})=0 \tag{6}$$

(3) periodic conditions:

$$\Phi'(\bar{a})=\Phi'(\bar{b}) \quad \text{and} \quad w_1\Phi''(\bar{a})-w_{n-1}\Phi''(\bar{b})=s_1\Phi'(\bar{a})+s_n\Phi'(\bar{b})$$

A constructive approach[16], using piecewise cubic Hermite polynomials as basic functions, allows verifying existence and uniqueness of a weighted *v*-spline, under the chosen boundary conditions.

Given Φ_i and m_i, $i = 1, \ldots, n$, the unique piecewise cubic function $\Phi(x)$, of C^1 regularity, satisfying $\Phi(x_i) = \Phi_i$ and $\Phi'(x_i) = m_i$, $i = 1, \ldots, n$, can be represented[17,18] as

$$\Phi(x)=\sum_{i=1}^{n}\Phi_i P_i(x) + m_i D_i(x) \tag{7}$$

where

$$P_i(x)=\begin{cases}(x-x_{i-1})^2[2(x_i-x)+h_{i-1}]/h_{i-1}^3 & x_{i-1}\le x\le x_i\\ (x_{i+1}-x)^2[2(x-x_i)+h_i]/h_i^3 & x_i<x\le x_{i+1}\\ 0 & \text{elsewhere}\end{cases}$$

$$D_i(x)=\begin{cases}(x-x_{i-1})^2(x-x_i)/h_{i-1}^2 & x_{i-1}\le x\le x_i\\ (x-x_{i+1})^2(x-x_i)/h_i^2 & x_i<x\le x_{i+1}\\ 0 & \text{elsewhere}\end{cases}$$

and $h_i = x_{i+1} - x_i$. Since functions $P_i(x)$ and $D_i(x)$ are null out of interval $[x_{i-1}, x_{i+1}]$, equation (7), for $x_i \le x \le x_{i+1}$, becomes

$$\Phi(x)=\Phi_i P_i(x) + m_i D_i(x) + \Phi_{i+1} P_{i+1}(x) + m_{i+1} D_{i+1}(x) \tag{8}$$

If in equation (7) coefficients m_i are considered as the unknowns, minimizing functional V in (5) implies solving equations:

$$\frac{\partial V(\Phi)}{\partial m_k}=0 \qquad k=2,\ldots,n-1. \tag{9}$$

By means of (5) and (7) we obtain[19]:

$$\begin{aligned}2c_{k-1}m_{k-1}+(s_k+4c_{k-1}+4c_k)m_k+2c_k m_{k+1}=\\ =6c_k(\Phi_{k+1}-\Phi_k)/h_k+6c_{k-1}(\Phi_k-\Phi_{k-1})/h_{k-1}\end{aligned} \tag{10}$$

for $k = 2, \ldots, n-1$, where $c_i = w_i/h_i$, w_i = constant.

The above $n - 2$ equations (10) involve n unknowns $m_1, \ldots, m_n$. Two more conditions are needed in order for the system to be closed. They are imposed by means of the spline boundary conditions, which can be of first kind, i.e.:

$$m_1 = \Phi'(\bar{a}) \qquad m_n = \Phi'(\bar{b})$$

or of second kind, i.e.:

$$(s_1+4c_1)m_1+2c_1m_2=6c_1(\Phi_2-\Phi_1)/h_1$$
$$2c_{n-1}m_{n-1}+(s_n+4c_{n-1})m_n=6c_{n-1}(\Phi_n-\Phi_{n-1})/h_{n-1}$$

or of third kind, i.e.:

$$\begin{aligned}(s_1+s_n+4c_1+4c_{n-1})m_1+2c_1m_2+2c_{n-1}m_{n-1}&=\\ =6c_1(\Phi_2-\Phi_1)/h_1+6c_{n-1}(\Phi_n-\Phi_{n-1})/h_{n-1}&\\ m_1=m_n&\end{aligned} \tag{11}$$

OUR NEW PROFILE

Very often, in what follows, we shall indicate a grid point x_i simply by its index i. We use weighted natural cubic v-splines to define a new profile for the dependent variable.

Consider an internal grid point and the volume relative to it (*Figure 1*). We build the weighted v-spline on interval $[i-1, i+1]$, thus obtaining a local profile for variable Φ involving values of such variable at three consecutive nodes. The convective nature of the differential equation suggests that the velocity direction, which from now on is considered positive, be taken into account; therefore our profile, used for determining the value of Φ on the right face of the control volume, involves values of Φ at nodes $i-1$, i, $i+1$. If the velocity were negative, the grid points to be used when determining Φ_r would be i, $i+1$, $i+2$ and the computations would be exactly the same as for the shifted points relative to positive velocity, considered in the opposite order.

To compute the derivatives m_i, $i = 1, \ldots, n$, we solve a system obtained from (10) by assuming the natural spline boundary conditions. We formally solve:

$$\begin{bmatrix} \frac{a}{h} & \frac{f}{2}+\frac{2a}{h}+\frac{2b}{k} & \frac{b}{k} \\ \frac{e}{2}+\frac{2a}{h} & \frac{a}{h} & 0 \\ 0 & \frac{b}{k} & \frac{g}{2}+\frac{2b}{k} \end{bmatrix} \begin{bmatrix} m_{i-1} \\ m_i \\ m_{i+1} \end{bmatrix} = \begin{bmatrix} A \\ B \\ C \end{bmatrix} \tag{12}$$

where

$a = w_{i-1}$ $\quad b = w_i$ $\quad e = s_{i-1}$ $\quad f = s_i$

$g = s_{i+1}$ $\quad h = x_i - x_{i-1}$ $\quad k = x_{i+1} - x_i$

$$A = \frac{3b}{k^2}\left(\Phi_{i+1}-\Phi_i\right)+\frac{3a}{h^2}\left(\Phi_i-\Phi_{i-1}\right)$$

$$B = \frac{3a}{h^2}\left(\Phi_i-\Phi_{i-1}\right) \qquad C = \frac{3b}{k^2}\left(\Phi_{i+1}-\Phi_i\right)$$

After solving such system, the first derivative at node $i+1$ can be written as:

$$m_{i+1} = \alpha_r\Phi_{i-1}+\beta_r\Phi_i+\gamma_r\Phi_{i+1} \tag{13}$$

where α_r, β_r, γ_r are coefficients depending on distances h and k and on the weight functions:

$$\begin{aligned}\alpha_r &= 2ak^2(2a+eh)/DEN\\ \beta_r &= [-(4a^2k(k+3h)+2ah(4bh+ek(k+2h)+2fkh))-eh^3(2b+fk)]/DEN\\ \gamma_r &= h(12a^2k+4ah(2b+k(e+f))+eh^2(2b+fk))/DEN\end{aligned} \tag{14}$$

$$DEN=[12a^2k(4b+gk)+4ah(12b^2+4b^2k(e+f+g)+gk^2(e+f))+eh^2(12b^2+4bk(f+g)+fgk^2)]\cdot\frac{kh}{6b}$$

From (12) and (13) we obtain:

$$\begin{aligned}m_i &= -\alpha_r\left(\frac{gk}{2b}+2\right)\Phi_{i-1}-\left[\frac{3}{k}+\beta_r\left(\frac{gk}{2b}+2\right)\right]\Phi_i+\left[\frac{3}{k}-\gamma_r\left(\frac{gk}{2b}+2\right)\right]\Phi_{i+1}\\ m_{i-1} &= \frac{1}{DN}\left[\left(T\alpha_r-\frac{3a}{h^2}\right)\Phi_{i-1}+\left(T\beta_r+\frac{3a}{h^2}+\frac{3a}{kh}\right)\Phi_i+\left(T\gamma_r-\frac{3a}{hk}\right)\Phi_{i+1}\right]\end{aligned} \tag{15}$$

where

$$T=\frac{a}{h}\left(\frac{gk}{2b}+2\right) \qquad DN=\frac{e}{2}+\frac{2a}{h}$$

The technique presented until now is in general used to interpolate pointwise known functions. The idea we exploit is, although the values Φ_i are not known, we express all the other quantities in terms of such values Φ_i and only subsequently, by the discretized differential equation, determine them.

After introducing a local co-ordinate system, interval $[i-1, i+1]$ becomes as in *Figure 2*. Since we are interested in the value of Φ_r, we need to consider the restriction of our v-spline to interval $[0, x_3]$, which is equivalent to considering the expression of Φ on interval $[i, i+1]$. This profile, by (8), is:

$$\Phi(x)=\Phi_2P_2(x)+m_2D_2(x)+\Phi_3P_3(x)+m_3D_3(x) \tag{16}$$

where the Hermite functions[18] become:

$$P_2(x)=\frac{(k-x)^2}{k^3}[2x+k] \qquad P_3(x)=\frac{x^2}{k^3}[3k-2x]$$

$$D_2(x)=\frac{x}{k^2}[x-k]^2 \qquad D_3(x)=\frac{x^2}{k^2}[x-k]$$

By evaluating (16) at $x = k/2$, we have:

$$\Phi_r=\Phi(k/2)=\frac{1}{2}\Phi_2+\frac{k}{8}m_2+\frac{1}{2}\Phi_3-\frac{k}{8}m_3 \tag{17}$$

Here derivatives m_2 *e* m_3 equal derivatives m_i and m_{i+1} previously quoted. Therefore our profile on the right face is:

$$\Phi_r=-D_r\alpha_r\Phi_{i-1}+\left(\frac{1}{8}-D_r\beta_r\right)\Phi_i+\left(\frac{7}{8}-D_r\gamma_r\right)\Phi_{i+1} \tag{18}$$

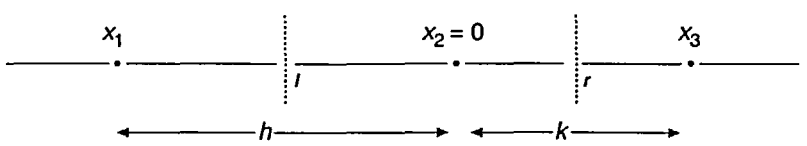

Figure 2 Local co-ordinate system involving nodes $i-1, i, i+1$

with $D_r = \frac{k}{8}\left(\frac{gk}{2b} + 3\right)$

In order to evaluate the first derivative, $\frac{\partial\Phi}{\partial x}\Big|_r$, on the right face we must differentiate Φ of eqn. (16) and find its value at $x = -\frac{k}{2}$. We obtain:

$$\left.\frac{\partial\Phi}{\partial x}\right|_r = -\frac{3}{2k}\Phi_i + \frac{3}{2k}\Phi_{i+1} - \frac{1}{4}m_i - \frac{1}{4}m_{i+1} = \\ = P_r\alpha_r\Phi_{i-1} + \left(P_r\beta_r - \frac{3}{4k}\right)\Phi_i + \left(P_r\gamma_r + \frac{3}{4k}\right)\Phi_{i+1} \tag{19}$$

with $P_r = \frac{kg}{8b} + \frac{1}{4}$

By what was described above we obtain a profile depending on the weights s_i and w_i. We remark that, by acting on such weights appropriately, the numerical solution can be handled in such a way that it enjoys some desired property. In a subsequent section we describe the study of the optimal choice of the weight coefficients which ensures a third order monotonic scheme.

By exploiting the choice of unequal volumes, allowed by the v-splines, moreover, we can formulate a method in which the volume sizes are chosen in such a way that the solution is followed as closely as possible.

NORMALIZED VARIABLE

For the control of the oscillatory behaviour of the solution in (16) we impose the profile to be monotonic; this is performed by studying the NVD, i.e. the diagram of our variable, normalized by the following transformation:

$$\overline{\Phi} = \frac{\Phi - \Phi_{i-1}}{\Phi_{i+1} - \Phi_{i-1}} \tag{20}$$

then

$$\Phi = (\Phi_{i+1} - \Phi_{i-1})\ \overline{\Phi} + \Phi_{i-1}. \tag{21}$$

By relation (20), links between the variables in approximation schemes are simplified since it is $\overline{\Phi}_{i+1} = 1$ and $\overline{\Phi}_{i-1} = 0$. This means that, while Φ_r depends on Φ_{i+1}, Φ_{i-1} and Φ_i, the normalized variable $\overline{\Phi}_r$ depends only on $\overline{\Phi}$; a normalized variable diagram, therefore, allows a graphic representation of the functional relation between the normalized value $\overline{\Phi}_r$ and the normalized value at the upstream node $\overline{\Phi}_i$.

If, for example, we think $u_r > 0$, the QUICK scheme is normalized as

$$\overline{\Phi}_r = \frac{1}{2}(1+\overline{\Phi}_i) - \frac{1}{8}(1-2\overline{\Phi}_{i+1}) \tag{22}$$

By replacing (20) in (18), we obtain:

$$(\Phi_{i+1} - \Phi_{i-1})\left\{\overline{\Phi}_r + D_r\alpha_r\ \overline{\Phi}_{i-1} - \left(\frac{1}{8} - D_r\beta_r\right)\overline{\Phi}_i - \left(\frac{7}{8} - D_r\gamma_r\right)\overline{\Phi}_{i+1}\right\} + \\ + \Phi_{i-1}\left\{1 + D_r\alpha_r - \frac{1}{8} + D_r\beta_r - \frac{7}{8} + D_r\gamma_r\right\} = 0 \tag{23}$$

and the coefficient of Φ_{i-1}, by simple computation, turns out to be null. Therefore, in normalized variables, (18) becomes:

$$\bar{\Phi}_r = \left(\frac{1}{8} - D_r\beta_r\right)\bar{\Phi}_i + \frac{7}{8} - D_r\gamma_r \tag{24}$$

In Leonard[20], NVD relative to the various known profiles are studied. This study led to stating the following criteria to verify validity of a scheme for equal volumes:

(1) a necessary and sufficient condition in order for the scheme to provide second order approximation is that its NVD includes point Q ∫ (1/2,3/4)

(2) a necessary and sufficient condition in order for the scheme to be of the third order is that the derivative at Q be 3/4.

These criteria hold for every functional relation, linear or non-linear. It has also been remarked that NVD lines in the second quadrant (negative abscissa, positive ordinate) are a feature of profiles with unrealistic oscillatory behaviour while NVD lines in the fourth quadrant (positive abscissa and negative ordinate) are typical of schemes generating numerical diffusion.

The Exponential Upwinding scheme[20], was developed exactly by considering these criteria: it assumes a local exponential behaviour for the variable and, in normalized variable, it yields a non-linear relation such as:

$$\bar{\Phi}_r = \frac{\sqrt{\bar{\Phi}_i\left(1-\bar{\Phi}_i\right)^3 - \bar{\Phi}_i^2}}{1-2\bar{\Phi}_i} \tag{25}$$

Since the two criteria above are verified by it, this scheme is of the third order; it has to be remarked, however, that its computational cost is very high and that it is convenient only when $0 \le \bar{\Phi}_i \le 1$. Out of such interval it has to be continued by means of other schemes such as QUICK or UPWIND. This kind of continuation is realized by algorithm EULER-QUICK and by its 2D version, SHARP[20].

An NVD analysis is the basis also of another recent algorithm, ULTIMATE, where the value $\bar{\Phi}_r$ is modified according to the universal limiter[13].

A NEW PROFILE: FAST (FLOW APPROXIMATION BY SPLINE TECHNIQUES)

We studied the general profile (24) in order to impose monotonicity. By using equal volumes and natural cubic splines (i.e. a = b = l, e = f = g = 0), our profile in NVD is:

$$\bar{\Phi}_r = \frac{1}{32}\left[\,22\ \bar{\Phi}_i + 13\,\right] \tag{26}$$

which is represented by a straight line including point Q, with angular coefficient at Q of 11/16; therefore (26) yields a second order scheme (criterion 1). If unequal volumes are used, in NVD, we have:

$$\bar{\Phi}_r = \frac{8v+3}{16v}\,\bar{\Phi}_i + \frac{8v+5}{16(1+v)} \tag{27}$$

This straight line, depending on the value of v, the ratio h/k of the sizes of two consecutive volumes, includes a general point Q, of abscissa 1/2, with a family of values of its ordinate (*Figure 3*). By imposing that the ordinate of Q be less than unity, so that the line keeps within the unit square, we obtain the condition $1/3<v<3$. Although the ordinate of Q can be different from 3/4 (which anyway is required only for schemes making use of equal volumes), the second order approximation is ensured, as can be seen in the next section.

We also studied our profile by assuming the volumes to be equal and including weight coefficients. Numerical experience[21], suggests that only three of the five weight coefficients should

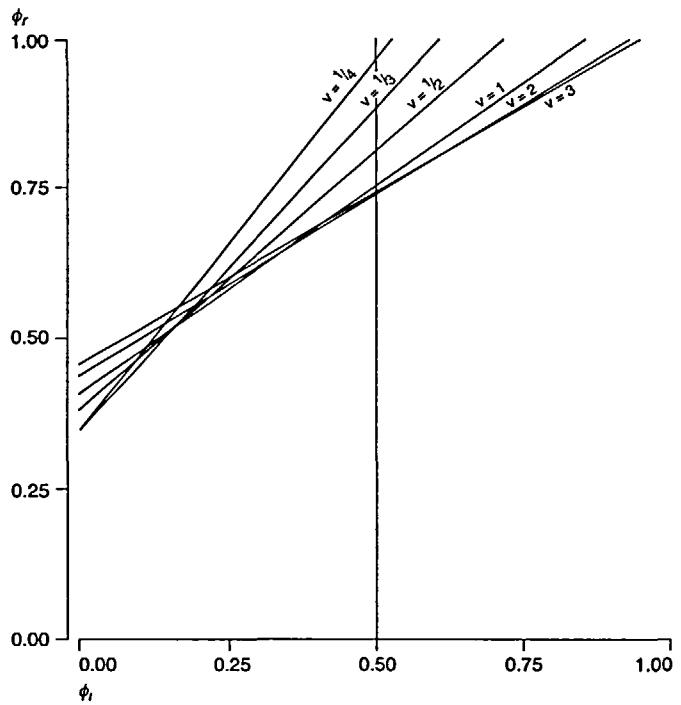

Figure 3 Natural cubic splines profile in NVD for unequal volumes

be considered: a, b and f. Varying weights e and g shows a very limited influence on the profile, so that we decided to set them both to zero:

$$e=g=0 \tag{28}$$

If we assign f proper values, we can control the first derivative of the cubic interpolation function at node i, while modifying coefficients a and b affects curvature in intervals $[i-1, i]$ and $[i, i+1]$. By this we obtain:

$$\bar{\Phi}_r = \frac{42a+24b+fh(2b+9)}{16(3a+3b+bfh)}\,\bar{\Phi}_l + \frac{15a+24b+fh(14b-9)}{16(3a+3b+bfh)} \tag{29}$$

Since we are assuming the volumes to be equal, criteria 1 and 2 are to be satisfied.

Let us therefore impose that the profile goes through Q = (1/2,3/4) and obtain the following conditions on the weight coefficients:

$$f=0 \qquad \text{or} \qquad b=3/2 \tag{30}$$

The first of the above conditions was chosen since it simplifies the profile expression.

If we impose the further condition that the diagram includes the origin, we obtain $a = -8b/3$ when $f = 0$ and $a = -4(3 + fh)/5$ when $b = 3/2$.

Results obtained for the aforementioned schemes were used to study the general profile (18) when both volume sizes and weight coefficients (only three of them) can vary. In NVD we obtain:

$$\bar{\Phi}_r = \frac{33av+24bv^2+2bfhv^2+9a+9fhv^2}{16v(3a+3bv+bfhv)}\,\bar{\Phi}_l + \frac{15a+24bv+14bfhv-9fhv}{16(3a+3bv+bfhv)}\,. \tag{31}$$

By imposing that at the general point $Q \equiv (0.5, \frac{21av + 24bv^2 + 3a}{32v(a + bv)})$ the derivative be 3/4 (criterion 2) a second condition on the weight coefficients is obtained:

$$b=a(3-v)/(4v^2) \tag{32}$$

Being b necessarily positive, this implies $0 < v < 3$, which confirms the already considered limitation on the ratio of consecutive volume sizes. Conditions (28),(30),(32), in profile (31) yield:

$$\bar{\Phi}_r = \frac{3}{4}\bar{\Phi}_i + \frac{v+2}{4(v+1)} \tag{33}$$

In the NVD of *Figure 4* this profile is represented by a bundle of straight lines, all with angular coefficient of 3/4, including the general point Q (depending on v). By transformation (21), profile (33) can be written in unnormalized variables, i.e.:

FAST
$$\Phi_r = -\frac{1}{4(v+1)}\Phi_{i-1} + \frac{3}{4}\Phi_i + \frac{v+2}{4(v+1)}\Phi_{i+1} \tag{34}$$

The graph in *Figure 4* shows that, if regularity conditions must be verified (for instance the null value at the origin) and if we desire a continuous profile in NVD, the profile can only be piecewise defined [22]. Our choice was:

$$\bar{\Phi}_r = \begin{cases} \dfrac{3(3v+5)}{4(v+1)}\bar{\Phi}_i & 0<\bar{\Phi}_i<1/6 \\ \dfrac{3}{4}\bar{\Phi}_i + \dfrac{v+2}{4(v+1)} & 1/6\le\bar{\Phi}_i\le(3v+2)/(3v+3) \\ 1 & (3v+2)/(3v+3)\le\bar{\Phi}_i\le 1 \end{cases} \tag{35}$$

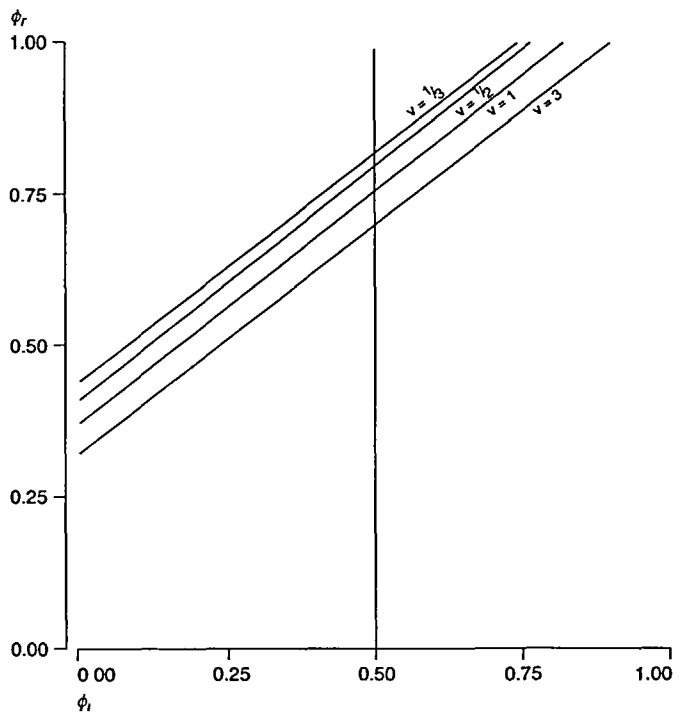

Figure 4 Weighted splines profiles in NVD for unequal volumes

with $\bar{\Phi}_r=\bar{\Phi}_1$ if $\bar{\Phi}_1\leq 0$ and $\bar{\Phi}_1\geq 1$.

Scheme (35) is used only in the unit square. Out of such square we adopt the UPWIND scheme. In *Figure 5* the NVD representation of FAST is given for various values of v.

TRUNCATION ERRORS

Analysis of the formal order of accuracy of our splines profile is based on Taylor series truncated expansions of variable Φ on the right face of the control volume:

$$\begin{aligned}
\Phi_{1-1}&=\Phi_r-(v_1+1/2)h\,\Phi_r'+(v_1+1/2)^2\frac{h^2}{2}\Phi_r''-(v_1+1/2)^3\frac{h^3}{6}\Phi_r'''+\ldots\\
\Phi_1&=\Phi_r-\frac{h}{2}\Phi_r'+\frac{h^2}{8}\Phi_r''-\frac{h^3}{48}\Phi_r'''+\ldots\\
\Phi_{1+1}&=\Phi_r+\frac{h}{2}\Phi_r'+\frac{h^2}{8}\Phi_r''+\frac{h^3}{48}\Phi_r'''+\ldots
\end{aligned} \tag{36}$$

By replacing these expansions in our profile we can find coefficients for the derivatives of Φ on face r, i.e. the scheme order on face r.

We follow a similar sequence as in the preceding section. In the case of equal volumes ($v_1 = 1$), without weights, after the proper simplifications, we have:

$$T.E.=-\frac{h^2}{32}\Phi_r''+O(h^3) \tag{37}$$

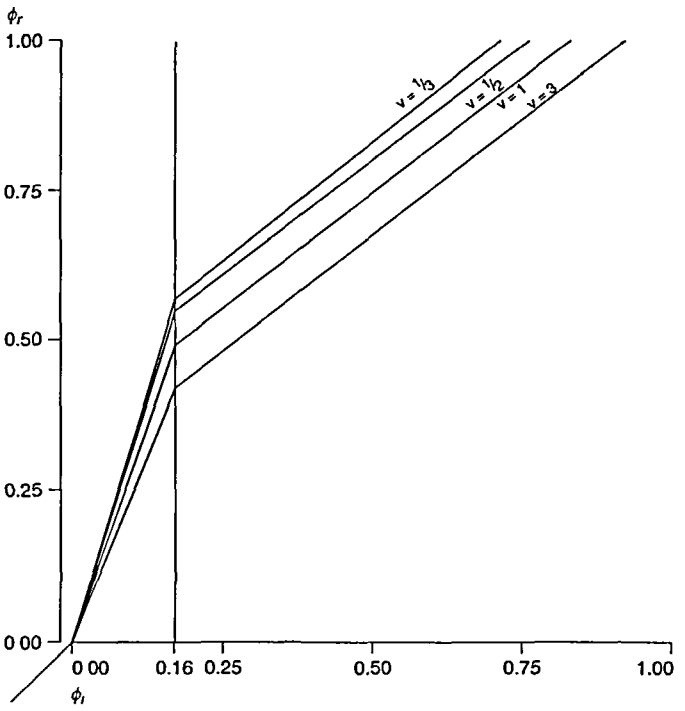

Figure 5 Profile FAST in NVD

For unequal volumes we get:

$$T.E.=\frac{h^2}{32}\,\Phi_r''+O(h^3) \tag{38}$$

For both the second order is ensured; we also point out that the coefficient of the second derivative turns out to be independent of v_1, i.e. the order of approximation is totally uninfluenced by changes in volume sizes. (Each time we mention unequal volumes, we refer to *Figure 1*.)

For the profile including weights *a*, *b* and *f*, with equal volumes, we have:

$$T.E.=\frac{h^2}{32(3a+3bv_1+bfhv_1)}\,[2fv_1(6b-9)\Phi_r'+(3a-9av_1+12bv_1+4bfhv_1)\Phi_r'']$$
$$+O(h^3) \tag{39}$$

once more of the second order.

We finally studied the local truncation error for profile FAST. By replacing expansions (36) in it we obtain:

$$\Phi_r=-\frac{1}{4(v_1+1)}\left[\Phi_r-(v_1+1/2)h\,\Phi_r'+(v_1+1/2)\frac{2h^2}{2}\Phi_r''-(v_1+1/2)\frac{3h^3}{6}\Phi_r'''+\ldots\right]$$
$$+\frac{3}{4}\left[\Phi_r-\frac{h}{2}\Phi_r'+\frac{h^2}{8}\Phi_r''-\frac{h^3}{48}\Phi_r'''+\ldots\right]$$
$$+\frac{v_1+2}{4(v_1+1)}\left[\Phi_r+\frac{h}{2}\Phi_r'+\frac{h^2}{8}\Phi_r''+\frac{h^3}{48}\Phi_r'''+\ldots\right]=$$
$$=\Phi_r+\frac{h^2(1-v_1)}{8}\Phi_r''+O(h^3)$$

so that

$$T.E.=\frac{h^2(1-v_1)}{8}\,\Phi_r''+O(h^3) \tag{40}$$

Profile FAST, therefore, gives a third order scheme for equal volumes ($v_1 = 1$), which reduces to the second order only at the volumes where a change in size occurs.

If we want to exploit the scheme at its best, then, it is required that the reduced volume size be maintained for a reasonable number of volumes (never less than 2) and that parameter v_1 be less than 2 in order for the coefficient of the second derivative to be as small as possible.

In equation (1) with $\Gamma = 0$ and $\rho = 1$ we obtain, for equal volumes, a spatial second order of approximation; by adopting an explicit time discretization scheme, we have:

$$\Phi_i^{n+1}=\Phi_i^n-c\,[\Phi_r^n-\Phi_l^n]=$$
$$=\Phi_i^n-c\left[\frac{1}{4(v_1+1)}\,\Phi_{i-2}^n-\frac{3v_2+4}{4(v_2+1)}\,\Phi_{i-1}^n+\frac{2v_1+1}{4(v_1+1)}\,\Phi_i^n+\right.$$
$$\left.+\frac{v_2+2}{4(v_2+1)}\,\Phi_{i+1}^n\right] \tag{41}$$

where $c=\dfrac{2\,u\,\Delta t}{h(v_2+1)}\,v_2$.

If we use the Taylor expansions (36) we obtain, after proper simplifications the following expression:

$$\Phi_1^{n+1} = \Phi_1^n - u\,\Delta t \left.\frac{\partial \Phi}{\partial x}\right|_1^n + \frac{u\,\Delta t\,h}{4v_2(1+v_2)}\left[-v_2^2(v_1+1)+(3v_2-2)(v_2+1)\right]\left.\frac{\partial^2\Phi}{\partial x^2}\right|_1^n +$$

$$+ \frac{u\,\Delta t\,h^2}{12v_2^2(1+v_2)}\left[v_2^3(v_1+1)^2-(3v_2^3+v_2^2-v_2+2)\right]\left.\frac{\partial^3\Phi}{\partial x^3}\right|_1^n. \tag{42}$$

The expansion of Φ_i^{n+1} with respect to time at Φ_i^n gives:

$$\Phi_1^{n+1} = \Phi_1^n + \Delta t \left.\frac{\partial \Phi}{\partial t}\right|_1^n + \frac{\Delta t^2}{2}\left.\frac{\partial^2\Phi}{\partial t^2}\right|_1^n + \frac{\Delta t^3}{6}\left.\frac{\partial^3\Phi}{\partial t^3}\right|_1^n. \tag{43}$$

if we equate the two expansions above, suppress indices and divide by Δt, we get:

$$\frac{\partial \Phi}{\partial t} + \frac{\Delta t}{2}\frac{\partial^2\Phi}{\partial t^2} + \frac{\Delta t}{6}\frac{\partial^3\Phi}{\partial t^3} + u\frac{\partial \Phi}{\partial x} +$$

$$- \frac{u\,h}{4v_2(1+v_2)}\left[-v_2^2(v_1+1)+(3v_2-2)(v_2+1)\right]\frac{\partial^2\Phi}{\partial x^2} +$$

$$- \frac{u\,h^2}{12v_2^2(1+v_2)}\left[v_2^3(v_1+1)^2-(3v_2^3+v_2^2-v_2+2)\right]\frac{\partial^3\Phi}{\partial x^3} = 0 \tag{44}$$

We now use the differential operator to eliminate the temporal derivative and, finally, obtain:

$$\frac{\Delta t}{2}u^2\frac{\partial^2\Phi}{\partial x^2} - \frac{\Delta t^2 u^3}{6}\frac{\partial^3\Phi}{\partial x^3} - \frac{u\,h}{4v_2(1+v_2)}\left[-v_2^2(v_1+1)+(3v_2-2)(v_2+1)\right]\frac{\partial^2\Phi}{\partial x^2} +$$

$$- \frac{u\,h^2}{12v_2^2(1+v_2)}\left[v_2^3(v_1+1)^2-(3v_2^3+v_2^2-v_2+2)\right]\frac{\partial^3\Phi}{\partial x^3} = 0 \tag{45}$$

For equal volumes we can recognize[23] a numerical dissipation coefficient of $\frac{\Delta t}{2}u^2$ and a numerical dispersion coefficient of $-\frac{\Delta t^2 u^3}{6} + \frac{uh^2}{8}$.

In equation (1) with $\Gamma \neq 0$, it can be more convenient to approximate the first derivative of Φ by a centred difference scheme instead of using the profile, as FV methods allow. By this approach the scheme turns out to be of second order.

VON NEUMANN STABILITY

Let us consider equation

$$\frac{\partial \Phi}{\partial t} = -u\frac{\partial \Phi}{\partial x} \tag{46}$$

By FV methods, if an explicit time discretization scheme is adopted, at node i we have:

$$\frac{\Phi_1^{n+1} - \Phi_1^n}{\Delta t} = -\frac{u}{\bar{A}}\left[\Phi_r^n - \Phi_1^n\right] \tag{47}$$

where A is the control volume size, $A = \frac{1+v_1}{2}h$ (*Figure 1*).

As can be seen in *Figure 1*, we are assuming the volumes are not necessarily equal. It should be remarked that, if the volumes are equal, all that follows holds and yields the stability region after setting $v_1 = v_2 = 1$ in all the quoted quantities.

The analysis we are going to perform should assume that, during the time advance, the solution being the superposition of wavetrains of different wave numbers, the components of the wavetrains "disperse", so that a non-uniform oscillatory wave is obtained, of approximate form $\Phi = \psi \exp(j\vartheta)$ (j imaginary unit), where ψ and the phase ϑ are functions of x and t and of the local, variable, wave number $k(x, t)$[24].

We are aware that this method is rather unusual, but we saw this as a reasonable way to study stability for unequal volumes.

We based our study on the application of the Finite Fourier Transform $\hat{\Phi}_l$ of the discretized solution Φ_i (i = 0, 1, 2, ... , M–1, with M number of grid points). By using variables as in Strickwerda[25], we have

$$\hat{\Phi}_l = \sum_0^{M-1} e^{-2\pi j i \frac{x_l}{L}} \Phi_i \tag{48}$$

where j is the imaginary unit, x_1 is the current abscissa and [0, L] is the domain.

We replace profile FAST in the scheme and obtain:

$$\Phi_i^{n+1} = \Phi_i^n - c\left[\frac{1}{4(v_1+1)}\Phi_{i-2}^n - \frac{3v_2+4}{4(v_2+1)}\Phi_{i-1}^n + \frac{2v_1+1}{4(v_1+1)}\Phi_i^n + \frac{v_2+2}{4(v_2+1)}\Phi_{i+1}^n\right] \tag{49}$$

where $v_1 = \Delta x_{i-1}/\Delta x_i$ and $v_2 = \Delta x_i/\Delta x_{i+1}$.

By inversion of Fourier Transform and its application in (49), we obtain

$$\hat{\Phi}_l^{n+1} = \hat{\Phi}_l^n \cdot G \tag{50}$$

where

$$G = 1 - c\left[\frac{1}{4(v_1+1)}\cos(2\vartheta) - \frac{1}{2}\cos(\vartheta) + \frac{2v_1+1}{4(v_1+1)}\right] + jc\left[\frac{1}{4(v_1+1)}\sin(2\vartheta) - \frac{2v_2+3}{2(v_2+1)}\sin(\vartheta)\right] \tag{51}$$

is the amplification factor[26], with $v = \frac{2\pi x_1}{L}$ and $c = \frac{u\Delta t}{A}$.

A necessary and sufficient condition in order for the scheme to be stable is $|G| \leq 1$.

By writing $|G|^2 \leq 1$ explicitly, we have:

$$1 - 2c\left[\frac{1}{4(v_1+1)}\cos(2\vartheta) - \frac{1}{2}\cos(\vartheta) + \frac{2v_1+1}{4(v_1+1)}\right] + c^2\left[\frac{1}{4(v_1+1)}\cos(2\vartheta) - \frac{1}{2}\cos(\vartheta) + \frac{2v_1+1}{4(v_1+1)}\right]^2 + c^2\left[\frac{1}{4(v_1+1)}\sin(2\vartheta) - \frac{2v_2+3}{2(v_2+1)}\sin(\vartheta)\right]^2 \leq 1, \tag{52}$$

whence, being $c > 0$,

$$c \le \frac{\frac{\cos(2\vartheta)}{2(v_1+1)} - \cos(\vartheta) + \frac{2v_1+1}{2(v_1+1)}}{\left[\frac{\cos(2\vartheta)}{4(v_1+1)} - \frac{\cos(\vartheta)}{2} + \frac{2v_1+1}{4(v_1+1)}\right]^2 + \left[\frac{\sin(2\vartheta)}{4(v_1+1)} - \frac{2v_2+3}{2(v_2+1)}\sin(\vartheta)\right]^2} \tag{53}$$

In the following figures the region of stability has been represented by plotting the right hand side $F(v_1, v_2, \vartheta)$ of the above inequality, interpreted as a function only of v_1 and ϑ and fixing several values of v_2.

The reason for choosing to give values to parameter v_2 was its lesser relevance with respect to the other two parameters. Indeed v_2 appears only in the ratio $(2v_2 + 3)/[2(v_2 + 1)]$, which always has a numerator equal to the denominator plus 1. The values we chose for v_2 were 1/3, 1/2, 1, 2: 1/3 because it represents a limitation of the domain for variable v_2 (see section on FAST); 1/2 and 2 because in actual computations we halve (double) the volume size when we want a closer study of the numerical solution (when the solution is smooth enough); 1 because it gives information relative to the uniform step situation.

The study of the surfaces above has been carried out for $c \in (0,0.6]$ and $\vartheta \in [0,2\pi]$.

In *Figure 6* the surface $F(v_1, 1/3, \vartheta)$ is plotted; in *Figure 7* the surface $F(v_1, 1/2, \vartheta)$; in *Figure 8* the surface $F(v_1, 1, \vartheta)$, in *Figure 9* the surface $F(v_1, 2, \vartheta)$.

A close observation and comparison of *Figures 6-9* shows the influence of both parameters v_1 and v_2 to be very limited. In particular, *Figure 8* relative to $v_2 = 1$, includes, at $v_1 = 1$ the stability region for equal volumes: is is easily seen that the surface is "almost" obtained by a rigid motion of $F(1, 1, \vartheta)$ along the v_1 axis, i.e. that changes in volume size do not lead to reduce the stability region.

The same kind of study has been performed for the parabolic equation

$$\frac{\partial \Phi}{\partial t} = - u\frac{\partial \Phi}{\partial x} + \Gamma \frac{\partial^2 \Phi}{\partial x^2} \, . \tag{54}$$

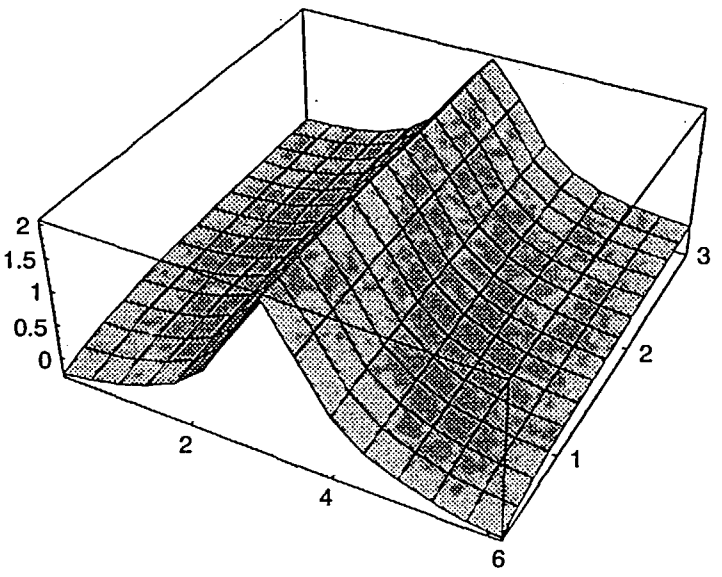

Figure 6 Stability region for the hyperbolic equation with $v_2 = 1/3$

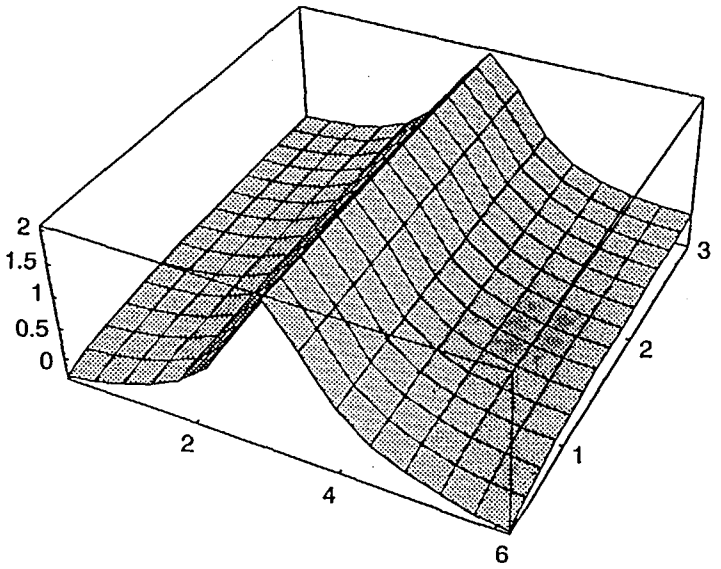

Figure 7 Stability region for the hyperbolic equation with $v_2 = 1/2$

In this case the scheme becomes:

$$\Phi_i^{n+1}=\Phi_i^n-c\left[\frac{1}{4(v_1+1)}\Phi_{i-2}^n-\frac{3v_2+4}{4(v_2+1)}\Phi_{i-1}^n+\frac{2v_1+1}{4(v_1+1)}\Phi_i^n+\frac{v_2+2}{4(v_2+1)}\Phi_{i+1}^n\right]+$$

$$+\frac{\Gamma\,\Delta t}{A}\left[v_2\,\frac{\Phi_{i+1}^n-\Phi_i^n}{h}-\frac{\Phi_i^n-\Phi_{i-1}^n}{h}\right] \tag{55}$$

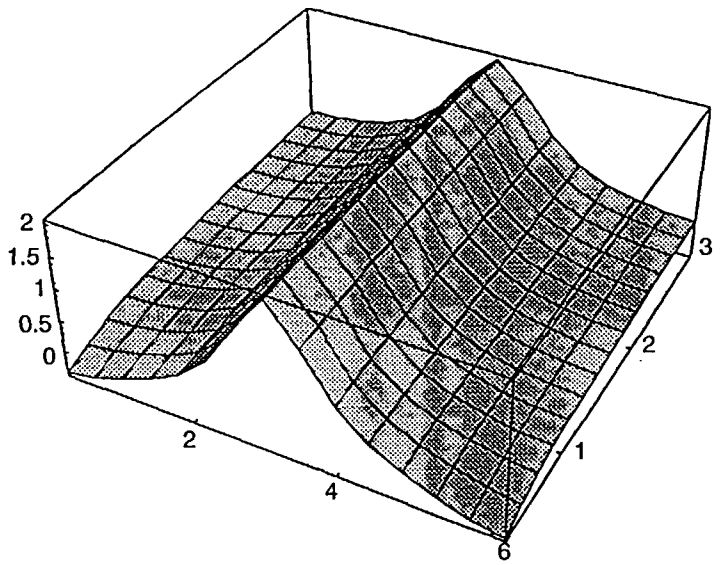

Figure 8 Stability region for the hyperbolic equation with $v_2 = 1$

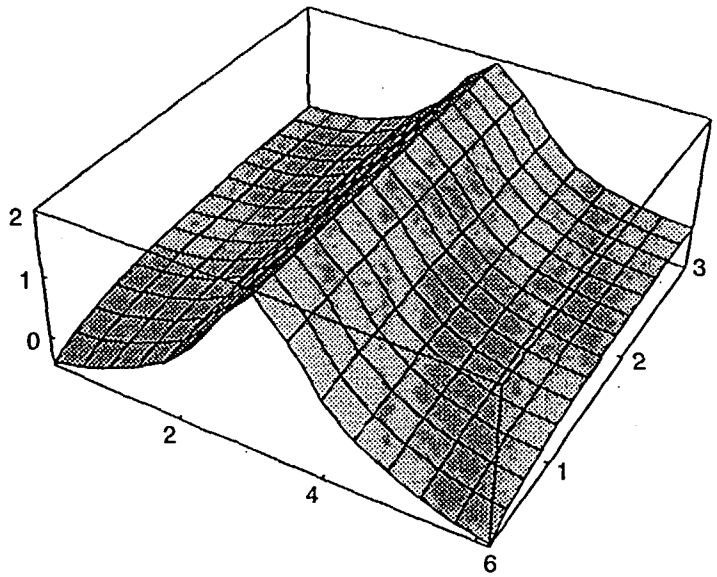

Figure 9 Stability region for the hyperbolic equation with $v_2 = 2$

so that G becomes:

$$G = 1 - c\left[\frac{1}{4(v_1+1)}\cos(2\vartheta) - \frac{1}{2}\cos(\vartheta) + \frac{2v_1+1}{4(v_1+1)}\right] + \frac{\Gamma\,\Delta t}{hA}\left[(v_2+1)\cos(\vartheta) - (v_2+1)\right] + jc\left[\frac{1}{4(v_1+1)}\sin(2\vartheta) - \frac{2v_2+3}{2(v_2+1)}\sin(\vartheta)\right] + \frac{\Gamma\,\Delta t}{hA}\, j\,(v_2-1)\sin(\vartheta). \tag{56}$$

We set $\alpha = \frac{\Gamma \Delta t}{hA}$. The necessary and sufficient condition, with both sides squared, becomes:

$$2\alpha^2\left(v_2^2+1-2v_2\cos(\vartheta)\right) - 2\alpha\left\{v_2+1-\frac{c}{2(v_1+1)(v_2+1)}\left[2v_2(v_2+1)\cos^2(\vartheta) + -(3v_1v_2^2+3v_1v_2+2v_2^2+3v_2-2v_1-1)\cos(\vartheta) - v_1v_2^2+v_1v_2+4v_1) - 2v_2^2-v_2+3\right]+ \frac{c^2}{4(v_1+1)^2(v_2+1)^2}\left\{(2v_1v_2^2+6v_1v_2+2v_2^2+6v_2+4v_1+4)\cos^2(\vartheta) + -(3v_1^2v_2^2+10v_1^2v_2+2v_1v_2^2+8v_1^2+10v_1v_2+2v_2+10v_1+3)\cos(\vartheta) + -(5v_1^2v_2^2+14v_1^2v_2+8v_1v_2^2+24v_1v_2+10v_1^2+4v_2^2+18v_1+12v_2+9)\right\} + c\,\frac{\cos(\vartheta)-v_1}{v_1+1} \le 0 \tag{57}$$

For equal volumes this reduces to:

$$4\alpha^2(1-\cos(\vartheta)) - 2\alpha\left\{2-\frac{c}{2}[\cos(\vartheta)-1]^2\right\} + - \frac{c^2}{8}\left\{3\cos^2(\vartheta)-6\cos(\vartheta)-13\right\}+c\frac{\cos(\vartheta)-1}{2}\leq 0 \tag{58}$$

If $\vartheta \neq 0$ and $\vartheta \neq 2\pi$, i.e. in the interior of the domain, the stability region is bounded by the surfaces of *Figure 10*. For $\vartheta = 0$ or $\vartheta = 2\pi$, inequality (58) degenerates into $\alpha \geq c^2/2$.

In order to represent the stability region by its lower and upper limitations, given by inequality (57), we considered some couples of values for parameters v_1 and v_2 and chose the most representative couples: (1, 1) (equal volumes) (*Figure 10*), (1, 2) (halving the second volume size) (*Figures 11* and *12* from different viewpoints)) and (2, 1) (halving the first volume size) (*Figure 13*).

PHASE ERRORS

By analysing the amplification factor G we can also study the phase error of the hyperbolic scheme, i.e. the positive or negative delay of the numerical solution with respect to the exact solution[27]. In a time-dependent convective problem, if the influence of boundary conditions is neglected, the exact solution can be written as

$$\Phi_k = \psi e^{j(\vartheta-kut)} = \psi e^{j(\vartheta-\omega t)} \tag{59}$$

where $k = k(x, t)$ is the local wave number, $\vartheta = \vartheta(k, \omega)$ is the local phase, $\omega = ku$ is the local frequency (u depending on k). The phase shift in the continuum is given as

$$\Delta\vartheta = -ku\ \Delta t = -kc\ A = -c\vartheta \tag{60}$$

with A the volume amplitude and Δt any time shift.

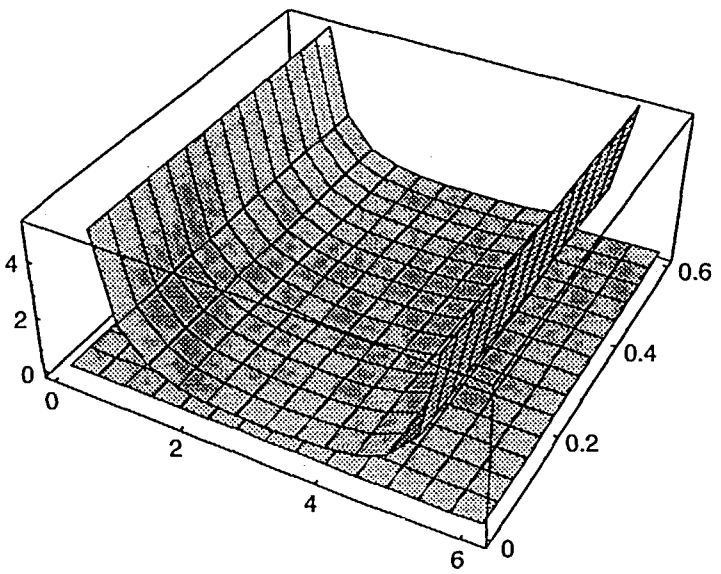

Figure 10 Stability region for the parabolic equation with $v_1 = v_2 - 1$

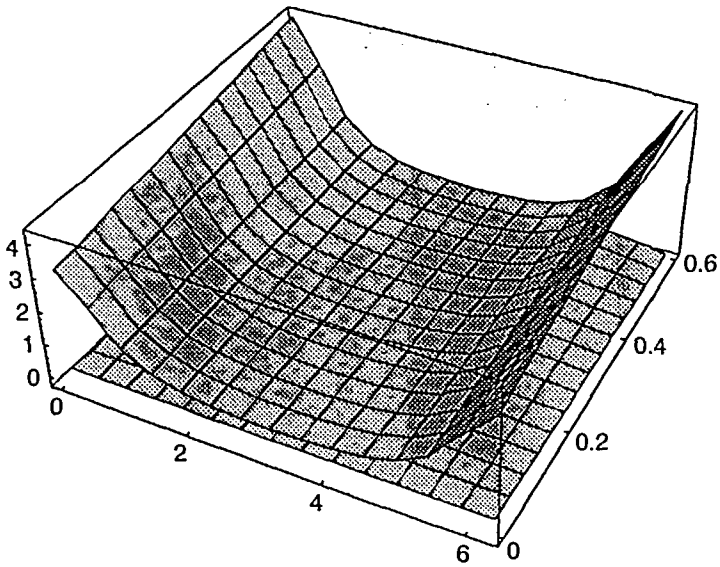

Figure 11 Stability region for the parabolic equation with $v_1 = 1$, $v_2 = 2$

In order to compute the phase error, (60) has to be compared with the numerical phase shift and this can be done by means of the amplification factor. From properties of polar co-ordinates we have:

$$\sin(\Delta\vartheta) = \frac{\mathrm{Imm}(G)}{|G|} \tag{61}$$

From (51) this becomes:

$$\mathrm{Imm}(G) = c\left[\frac{1}{4(v_1+1)}\sin(2\vartheta) - \frac{2v_2+3}{2(v_2+1)}\sin(\vartheta)\right] \tag{62}$$

$$|G|^2 = \left[1 - c\left(\cos(2\vartheta)/(4(v_1+1)) - \cos(\vartheta)/2 + (2v_1+1)/(4(v_1+1))\right)\right]^2 +$$

$$+ c^2\left[(\sin(2\vartheta)/(4(v_1+1)) - (2v_2+3)\sin(\vartheta)/(2(v_2+1))\right]^2 . \tag{63}$$

If $\Delta\vartheta$ is small enough, $\sin(\Delta\vartheta) \sim \Delta\vartheta$, so that we obtain:

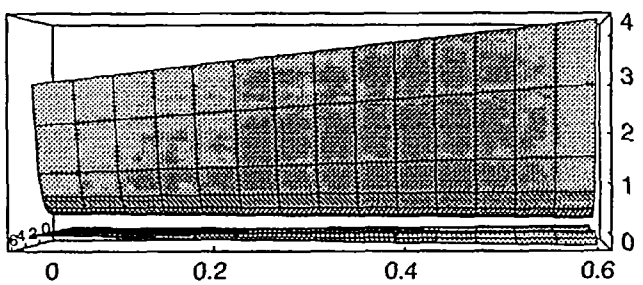

Figure 12 The same stability region from a different viewpoint

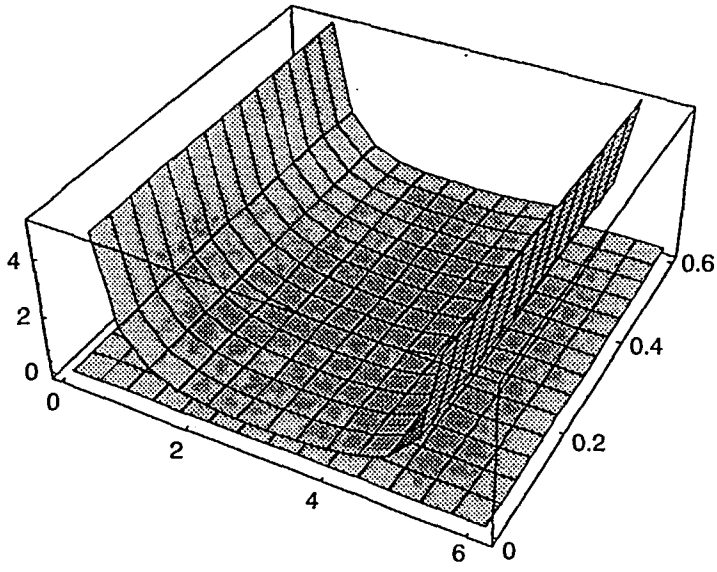

Figure 13 Stability region for the parabolic equation with $v_1 = 2$, $v_2 = 1$

$$\Delta\vartheta = \frac{c\left[\sin(2\vartheta)/(4(v_1+1)) - (2v_2+3)\sin(\vartheta)/(2(v_2+1))\right]}{|G|} \propto$$

$$\propto c\vartheta\left[\left(\frac{1}{2(v_1+1)} - \frac{2v_2+3}{2(v_2+1)}\right) + \left(\frac{2v_2+3}{12(v_2+1)} - \frac{1}{3(v_1+1)}\right)\vartheta^2 + \left(\frac{1}{15(v_1+1)} - \frac{2v_2+3}{240(v_2+1)}\right)\vartheta^3 + O(\vartheta^6)\right] \tag{64}$$

Therefore the phase error r is:

$$r = \left(\frac{1}{2(v_1+1)} - \frac{2v_2+3}{2(v_2+1)}\right) + \left(\frac{2v_2+3}{12(v_2+1)} - \frac{1}{3(v_1+1)}\right)\vartheta^2 + \left(\frac{1}{15(v_1+1)} - \frac{2v_2+3}{240(v_2+1)}\right)\vartheta^3 + O(\vartheta^6) \tag{65}$$

If only the leading part of this error is considered, we get

$$r = -1 + \frac{v_2 - v_1}{2(v_1+1)(v_2+1)} + O(\vartheta^2) \tag{66}$$

The study of this form of r leads to the following considerations: first of all, the phase error depends on changes in the volume size. If such size remains constant ($v_1 = v_2 = 1$), the phase factor r is proportional to $\Delta\vartheta^2$:

$$r = -1 + 1/24\ \vartheta^2 + O(\vartheta^4) \tag{67}$$

If, on the contrary, there is some change in the volume size, factor r in (66) is composed of a constant part μ multiple of 1/8 and a part proportional to $\Delta\vartheta^2$, i.e. to h^2. If for example $v_1 = 1$ and $v_2 = 3$, it is (*Figure 2*)

$$r=-7/8+ \quad 1/48 \ \vartheta^2+O(\vartheta^4) \tag{68}$$

For $v_1 = 3$ and $v_2 = 1$, we have:

$$r=-9/8+ \ 1/8 \ \vartheta^2+O(\vartheta^4) \tag{69}$$

Therefore r has values greater or less than –1 depending on the ratios v_1 and v_2 of consecutive volume sizes.

It can be remarked that the constant part μ, multiple of 1/8, can be compensated when size variations opposite to those determining it occur. For $v_1 = 1$ and $v_2 = 3$, in fact, we have $\mu = -1 + 1/8$, while for $v_1 = 3$ and $v_2 = 1$ it is $\mu = -1-1/8$. This property could be taken advantage of profitably when formulating adaptive methods.

PHYSICALLY REALISTIC SOLUTIONS: PATANKAR RULES

Four rules, described by Patankar[11], grant a stable convergence of a FV algorithm to a physically realistic solution. If in the discretized stationary equation (55) we replace profile FAST for the convective term and a central approximation of second order for the diffusive term, we obtain:

$$A_1\Phi_1=A_{1-2}\Phi_{1-2}+ A_{1-1}\Phi_{1-1}+ A_{1+1}\Phi_{1+1}+ B_1 \tag{70}$$

where $A_i, A_{i-1}, A_{i-2}, A_{i+1}$ are coefficients of Φ at the corresponding nodes and B_i is the source term, with values:

$$A_1=u\,\frac{2v_1+1}{4(v_1+1)} + \Gamma\,\frac{v_2+1}{h} \qquad A_{1-2}= -\frac{u}{4(v_1+1)}$$

$$A_{1-1}= u\,\frac{3v_2+4}{4(v_2+1)} + \frac{\Gamma}{h} \qquad A_{1+1}= -u\,\frac{v_2+2}{4(v_2+1)} + \frac{\Gamma}{h}v_2 \tag{71}$$

$$B_1= \frac{1}{2}\ h\ S_1\frac{1+v_2}{v_2}$$

We confront this scheme, applied to equation (55), with respect to the following four criteria:

- Rule 1: Consistence on the faces of the control volume. When a face is in common between two adjacent volumes, the flux through it must be represented identically for the two volumes in the discretized equation. This means that the flux leaving a given volume through a particular surface is exactly the same as that which enters the adjacent volume through the same surface, i. e. $\Phi_l\,(i + 1) = \Phi_r\,(i)$. In FAST this condition is verified.
- Rule 2: Positive coefficients in the discretized equation. The value of variable Φ at a grid point is related to the values of Φ at the grid points close to it. If, therefore, all conditions in the problem remain unaltered, whenever Φ increases at a grid point, it must increase also at the grid points in the vicinity (think, e.g. of heat equation).

  By applying this rule to FAST, we notice that A_i and A_{i-1} are always positive, A_{i+1} can be positive under proper conditions on the quantities appearing in it, while A_{i-2} is always negative. This disadvantage, however, can be overcome in a time-dependent problem by partitioning coefficients in such a way that a positive part can be isolated and that the matrix of the algebraic system relative to 1D problems becomes tridiagonal[28].
- Rule 3: A correspondence between the coefficients. The coefficient relative to the node at study must equal the sum of the coefficients relative to the neighbouring nodes, i.e.

$$A_i = A_{i-2} + A_{i-1} + A_{i+1}. \tag{72}$$

This implies that the coefficient at the central grid point i is a weighted average of coefficients at the neighbouring grid points. By looking at coefficients (71), it is easily seen that the required relation is verified.

- Rule 4: Negative slope for the source term. Coefficient A_i can be made negative when linearizing B_i: therefore we have to require that the linearization coefficient for B_i be negative in order for the solution not to become physically unrealistic. In the problems we have studied no approximation of the source term was needed.

NUMERICAL EXPERIENCE

Profile FAST has been tested on two equation types: the stationary parabolic and the hyperbolic. The numerical solution was computed on a grid of points defined on the unit interval. The control volumes were defined by putting their faces at mid-distances between consecutive grid points. For the stationary equation the case test, proposed by Leonard[29] is:

$$u \frac{\partial \Phi}{\partial x} = \Gamma \frac{\partial^2 \Phi}{\partial x^2} + S(x) \tag{73}$$

with
$$S(x) = \begin{cases} 10-50x & 0 \le x \le 0.3 \\ 50x-20 & 0.3 \le x \le 0.4 \\ 0 & 0.4 \le x \le 1 \end{cases}$$

and with Dirichlet boundary conditions: $\Phi(0) = 0$ and $\Phi(1) = 0.1$.

This problem is of significance in the study of convection-diffusion problems because of the source term: actually most of the classical schemes for convective terms (CDS, EDS,...) give accurate solutions only if no source term is present. With the source term $S(x)$ above, moreover, the solution follows three different behaviours on the domain: quadratic, constant and exponential.

Numerical results, presented in *Figure 14* (Pe = 5) and *Figure 15* (Pe = 10), were obtained by a reduction in volume size where the solution is exponential. On interval [0, 1] we used 31 volumes with initial volume size $\Delta x = 0.05$ which is halved three times in the final part of the interval.

In *Figure 16* we give results obtained by means of QUICK for the same number of volumes, 31, and physical conditions (Pe = 10). As can be seen, there remains an oscillatory behaviour, with maximum error at the last grid point.

FAST was also implemented on three benchmark problems[13], obtained as the solutions of an advection unsteady 1D equation:

$$\frac{\partial \Phi}{\partial t} + u \frac{\partial \Phi}{\partial x} = 0 \tag{74}$$

with Dirichlet boundary conditions.

The first test problem deals with a piecewise constant function, with a jump:

$$\Phi(x,t) = \begin{cases} 1 & 0 \le x \le 0.2+t \\ 0 & x > 0.2+t \end{cases} \tag{75}$$

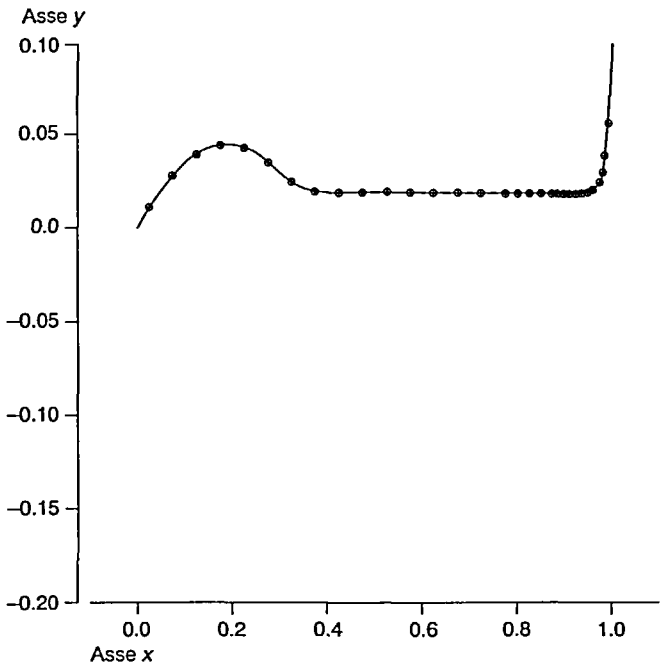

Figure 14 FAST solution for equation (73), Pe = 5, 31 volumes

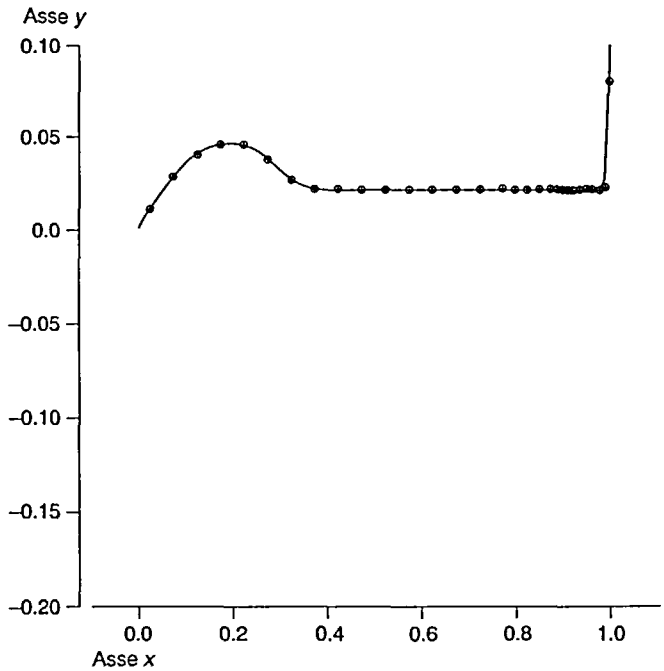

Figure 15 FAST solution for equation (73), Pe = 10, 31 volumes

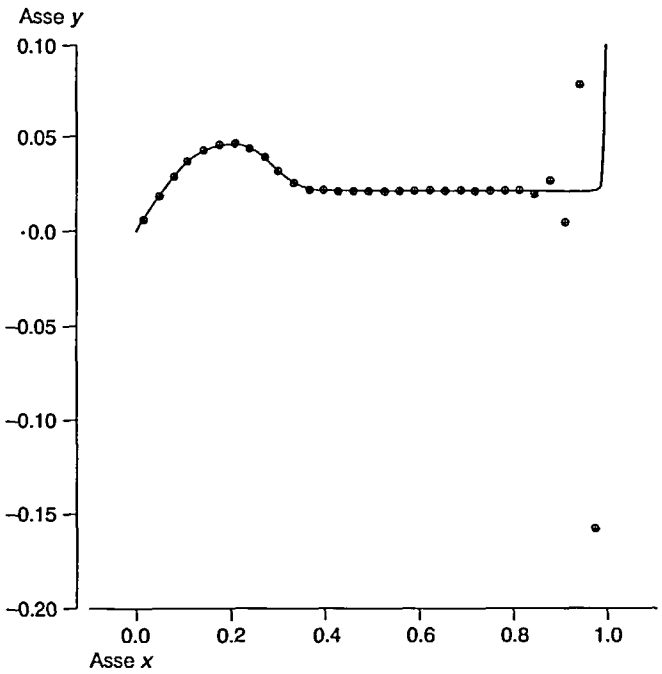

Figure 16 QUICK solution for equation (73), Pe = 10, 31 volumes

The second deals with an isolated wave, given by a squared sinum, which has continuous gradient:

$$\Phi(x,t)=\begin{cases}\sin^2\left(\dfrac{\pi(x-ut)}{0.2}\right) & t\le x\le 0.2+t\\ 0 & \text{elsewhere}\end{cases} \tag{76}$$

The third problem deals with a half ellipse, which combines continuous and discontinuous changes in the gradient:

$$\Phi(x,t)=\begin{cases}\sqrt{1-\dfrac{(x-ut-0.1)^2}{0.01}} & t\le x\le 0.2+t\\ 0 & \text{elsewhere}\end{cases} \tag{77}$$

Numerical examples were obtained for $c = 0.05$, with refinements in volume size near the discontinuity points; we used 76 volumes for the jump function, 77 for the other two.

By imposing monotonicity it was possible to avoid oscillatory behaviours completely and to obtain a satisfactory simulation of the exact solution with a numerical solution shown in *Figures 17, 18* and *19* after 900 time steps. *Figure 20* gives results for the jump function obtained by means of EULER-QUICK with 100 volumes. We performed several tests with various values of the Courant number c and, as forecast by the theoretical study, verified the method to be stable for values of $c \le 0.6$.

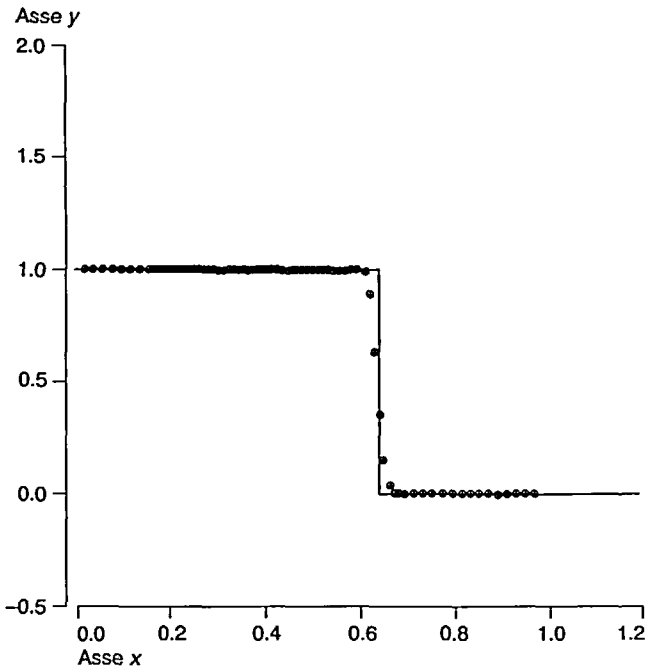

Figure 17 FAST solution for problem (75), 77 volumes, $c = 0.05$

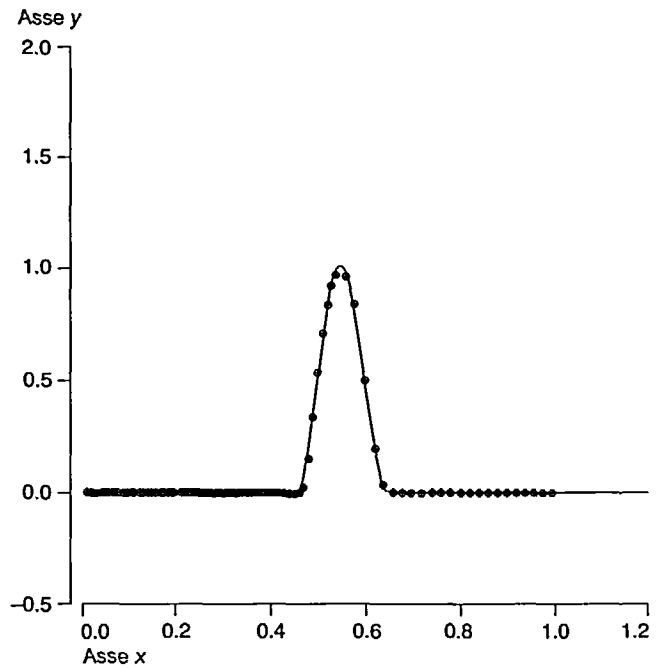

Figure 18 FAST solution for problem (77), 77 volumes, $c = 0.05$

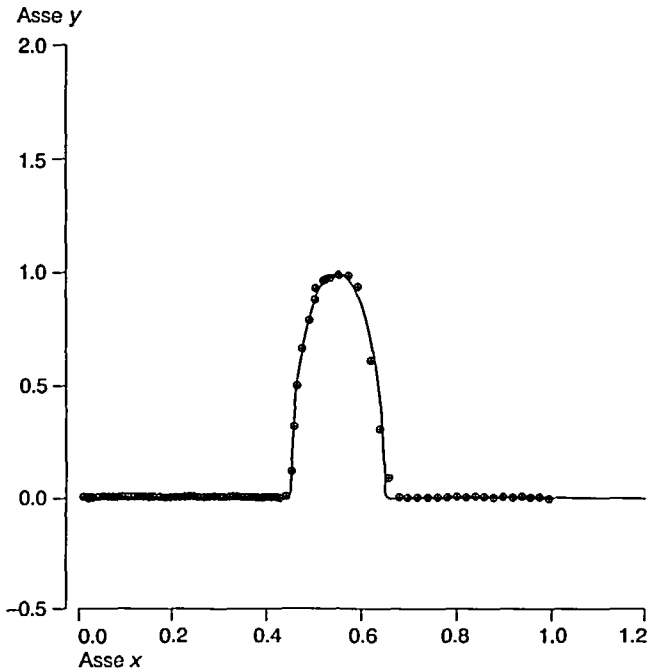

Figure 19 FAST solution for problem (77), 77 volumes, $c = 0.05$

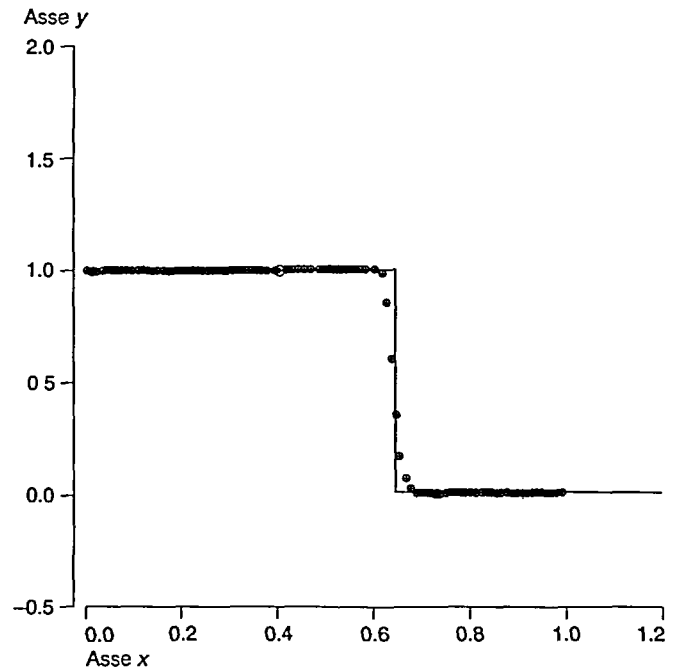

Figure 20 EULER-QUICK solution for problem (75), 100 volumes, $c = 0.05$

CONCLUSION

In this paper a new FV method has been presented, based on a profile, named FAST, obtained by means of weighted cubic v-splines for 1D parabolic and hyperbolic problems, with possible changes in the volume size. The study of a normalized variable allows an optimal definition of the weights in such a way that the order of approximation can be controlled and monotonicity can be imposed. The study of truncation errors shows that the method is of the third order (which reduces to the second at a volume where a change in size occurs).

Patankar's criteria to grant physically realistic solutions have been verified. Properties of stability and phase shift are formally analysed and numerically tested by means of some benchmark problems. An extension of the method capable of dealing with large Δt can be devised by similar reasoning as in Leonard *et al.*[30] and Roache[31].

Particularly good results are obtained by combining the accuracy of the proposed profile with a careful choice of the volume sizes: namely a smaller (halved) size can be used in the regions where the solution has discontinuities or high gradients.

Simplicity and generality of profile FAST, obtained by weighted cubic v-splines, suggest that the method can be extended for the solution of 2D or 3D convection-diffusion equations in fluid dynamics.

This extension could be performed both by simple operator splitting using 1D formulae or the same philosophy described in this paper could be followed by the definition of a 2D or 3D v-spline; in this latter approach, several weighting coefficients are to be defined. This, of course, implies a certain amount of computation, but it also implies that the approximation is extremely flexible and accurate.

ACKNOWLEDGEMENTS

The authors are deeply indebted to Dr S. Corti for valuable comments and suggestions in the study of phase errors. Sincere thanks also to the reviewers of the paper for their kind suggestions.

REFERENCES

1 Hirsch. C., Numerical Computation of Internal and External Flows, *Vol. 1: Fundamentals of Numerical Discretization*, J. Wiley & Sons, New York (1988)
2 Vinokur, M., An analysis of finite-difference and finite-volume formulations of conservation laws, *J. Comput. Phys.* **81**, 1-52 (1989)
3 Schreiber, W.C., Huang, C.L. and Chuan, C.H., The numerical solution of heat conduction in arbitrary shapes using the finite volume method with non-orthogonal grids, *Numerical Methods in Thermal Problems*, Vol. IV Part 2, Pineridge Press, Swansea (1989)
4 Maliska, C.R. and Raithby, G.D., A method for computing three dimensional flows using non-orthogonal boundary fitted co-ordinates, *Int. J. for Numer. Methods in Fluids*, Vol. 4, 519-537 (1984)
5 Baliga, B.R. and Patankar, S.V., A control volume finite-element method for two-dimensional fluid flow and heat transfer, *Numer. Heat Transfer*, Vol. 6, 245-261 (1983)
6 Schneider, G.E. and Raw, M.J., Control volume finite-element method for heat transfer and fluid flow using colocated variables, 1. Computational procedure, *Numer. Heat Transfer*, Vol. 11, 363-390 (1987)
7 Prakash, C. and Patankar, S.V., A control volume finite-element method for predicting flow and heat transfer in ducts of arbitrary cross sections – Part 1: Description of the method, *Numer. Heat Transfer*, Vol 12, 389-412 (1987)
8 Raithby, G.D., Skew upstream differencing schemes for problems involving fluid flow, *Comput. Methods Appl. Mech. Engrg*, **9**, 153-164 (1976)
9 Spalding, D.B., A novel finite difference formulation for differential expressions involving both first and second derivatives, *Int. J. Numer. Methods Eng.*, Vol. 4, 551-559 (1972)
10 Raithby, G.D. and Schneider, G.E., Elliptic systems: finite difference method II, *Handbook of Numerical Heat Transfer*, J. Wiley & Sons, New York (1988)
11 Patankar, S.V., *Numerical Heat Transfer and Fluid Flow*, Hemisphere, Washington (1980)
12 Leonard, B.P., A stable and accurate convective modelling procedure based on quadratic upstream interpolation, *Comput. Methods Appl. Mech. Engrg*, **19**, 59-98 (1979)

13 Leonard, B.P., The ULTIMATE conservative difference scheme applied to unsteady one-dimensional advection, *Comput. Methods Appl. Mech. Engrg*, **88**, 17-74 (1991)
14 Pennati, V., De Biase, L. and Marelli, M., New FV methods with v-splines approximation of profiles, *VIII International Conference on Numerical Methods for Thermal Problems*, Swansea, 11-16 July 1993
15 Casper, J. and Atkins, H.L., A finite-volume high-order ENO scheme for two-dimensional hyperbolic systems, *J. Comp. Phys*, **106**, 62-76 (1993)
16 De Boor, C., *A Practical Guide to Splines*, Springer-Verlag, New York (1978)
17 Prenter, P.M., *Splines and Variational Methods*, John Wiley & Sons, New York and Chichester (1975)
18 Cugiani, M., Metodi dell'Analisi Numerica, *UTET* (1977)
19 Foley, T.H., Interpolation with internal and point tension controls using cubic weighted v-splines, *ACM Transactions on Mathematical Software*, Vol. 13 No. 1, 68-96 (March 1987)
20 Leonard, B.P., Simple high-accuracy resolution program for convective modelling of discontinuities, *Int. J. for Numer. Methods in Fluids*, Vol. 8, 1291-1318 (1988)
21 Marelli, M., Metodi numerici avanzati per la soluzione di problemi differenziali in fluidodinamica", *ENEL CRIS, Rel.int*, No. 4548 (November 1992)
22 Zhu, J., On the higher-order bounded discretization schemes for finite volume computations of incompressible flows, *Comput. Methods Appl. Mech. Engrg*, **98**, 345-360 (1992)
23 Weylan, T., *Shallow Water Hydrodynamics*, Elsevier, Amsterdam (1992)
24 Whitham, G.B., *Linear and Nonlinear Waves*, J. Wiley & Sons, New York (1974)
25 Strickwerda, J.C., *Finite Difference Schemes and Partial Differential Equations*, Wadsworth & Brooks/Cole Math. Series (1989)
26 Smith, G.D., *Numerical Solution of Partial Differential Equation*, Claredon Press, Oxford (1985)
27 Roache, P.J., *Computational Fluid Dynamics*, Hermosa Publishers, Albuquerque (1972)
28 Hayase, T., Humphrey, J.A.C. and Greif, R., A consistently formulated QUICK scheme for fast and stable convergence using finite-volume iterative calculation procedures, *J. Comput. Phys*, **98**, 108-118 (1992)
29 Leonard, B.P. and Mokhtari, S., Beyond first-order upwinding: the ULTRA-SHARP alternative for non-oscillatory steady state simulation of convection, *Int. J. Numer. Methods Eng*, Vol. 30, 729-766 (1990)
30 Leonard, B.P., Lock, A.P. and Macvean, M.K., The NIRVANA scheme applied to unsteady one-dimensional advection, *Int. J. for Numer. Meth. in Heat and Fluid Flow*, **5**, 341-377 (1995)
31 Roache, P.J., A flux-based modified method of characteristics, *Int. J. for Numer. Meth. in Fluids*, **15**, 1259-1275 (1992)